ACS Chemical Neuroscience

pubs.acs.org/chemneuro Research Article

Stimulus-Specific Adaptation in Auditory Thalamus Is Modulated by the Thalamic Reticular Nucleus

Guoqiang Jia, Xinjian Li, Chunhua Liu, Jufang He,* and Lixia Gao*

Cite This: *ACS Chem. Neurosci.* 2021, 12, 1688−1697 Read Online

ACCESS | Metrics & More | Article Recommendations

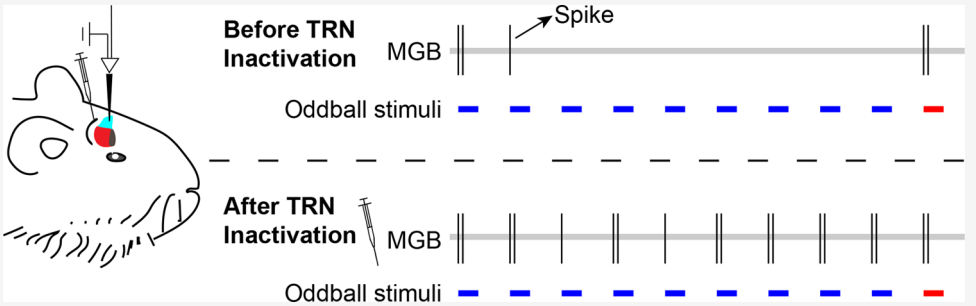

ABSTRACT: A striking property of the auditory system is its capacity for the stimulus-specific adaptation (SSA), which is the reduction of neural response to repeated stimuli but a recuperative response to novel stimuli. SSA is found in both the medial geniculate body (MGB) and thalamic reticular nucleus (TRN). However, it remains unknown whether the SSA of MGB neurons is modulated by inhibitory inputs from the TRN, as it is difficult to investigate using the extracellular recording method. In the present study, we performed intracellular recordings in the MGB of anesthetized guinea pigs and examined whether and how the TRN modulates the SSA of MGB neurons with inhibitory inputs. This was accomplished by using microinjection of lidocaine to inactivate the neural activity of the TRN. We found that (1) MGB neurons with hyperpolarized membrane potentials exhibited SSA at both the spiking and subthreshold levels; (2) SSA of MGB neurons depends on the interstimulus interval (ISI), where a shorter ISI results in stronger SSA; and (3) the long-lasting hyperpolarization of MGB neurons decreased after the burst firing of the TRN was inactivated. As a result, SSA of these MGB neurons was diminished after inactivation of the TRN. Taken together, our results revealed that the SSA of the MGB is strongly modulated by the neural activity of the TRN, which suggests an alternative circuit mechanism underlying the SSA of the auditory thalamus.

KEYWORDS: *Stimulus-specific adaptation (SSA), medial geniculate body (MGB), thalamic reticular nucleus (TRN), oddball procedure, intracellular recording, long-lasting hyperpolarization*

INTRODUCTION

The ability for mammals to detect a novel object or stimulus has been demonstrated at the single neuron level in several different sensory systems;[1−7] these systems function as a sensory filter or gain control in processing sensory information. Stimulus-specific adaptation (SSA), defined as the selective reduction of neural response to repetitive stimuli (standard stimuli) and recuperative response to a novel stimulus (deviant stimulus), has been proposed to be related to novelty detection and plays an important role in sound processing.[8] The SSA is strong and widespread in the auditory system, being found in most auditory neurons along the ascending auditory pathway from the midbrain up to the auditory cortex, such as the inferior colliculus (IC),[6,9−19] medial geniculate body (MGB),[20−26] thalamic reticular nucleus (TRN),[27,28] and auditory cortex.[7,29−36]

The MGB is the last obligate relay station in the auditory system, which comprises several subdivisions.[37−45] In general, the MGB is composed of ventral (MGV), dorsal (MGD), and medial subdivisions (MGM) based on response latency, firing patterns, and frequency-tuning properties, as well as different expression levels of neurotransmitters and neuromodulators.[41,44,46−52] Intracellular recording studies have revealed that MGV neurons respond to acoustic stimulation with excitatory postsynaptic potentials (EPSPs) superimposed with spikes at the peak of depolarization, whereas MGD neurons exhibited spikes followed by inhibitory postsynaptic potentials (IPSPs) or long-lasting IPSPs alone without a spiking response

Received: March 10, 2021
Accepted: April 12, 2021
Published: April 26, 2021

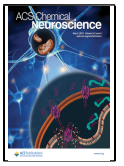

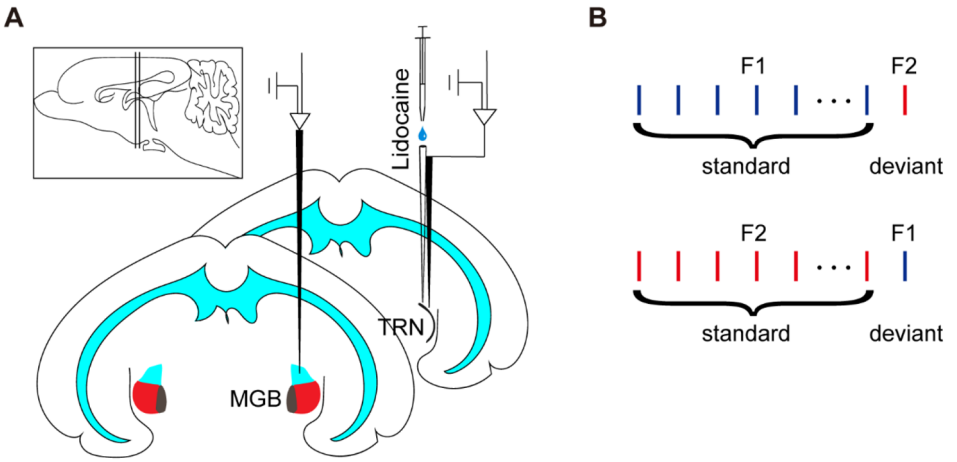

Figure 1. Illustration of experiment design. (A) Intracellular recordings in MGB of anesthetized guinea pig before and after inactivation of TRN via microinjection of lidocaine. The location of TRN was identified by extracellular recordings. The glass pipet for microinjection was glued to the tungsten electrode. The distance between the tips of the glass pipet and the tungsten electrode was less than 0.5 mm. The left top shows the relative location of MGB and TRN in the coronal plane. (B) Schematic illustrations of two oddball sequences, which consisted of standard and deviant tones; the frequency and ratio of the two tones are described in the Methods section.

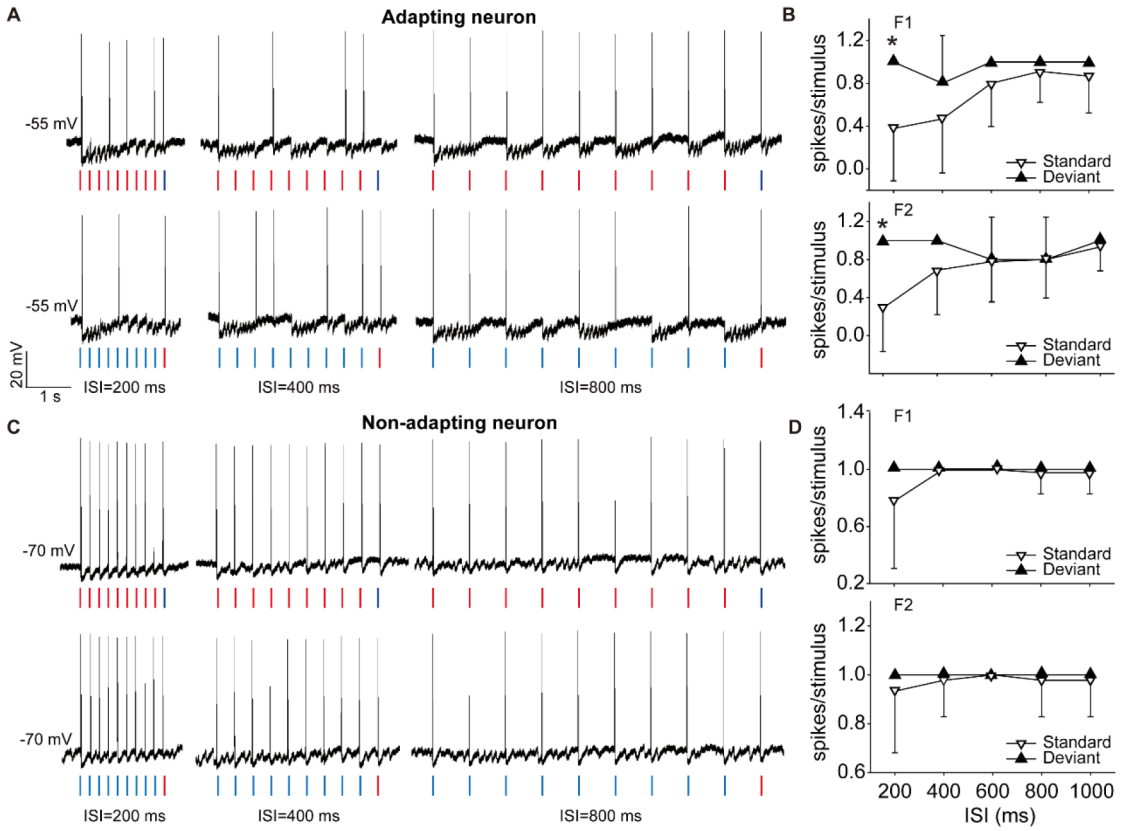

Figure 2. Adapting and nonadapting neurons in MGB. (A) An example MGB neuron demonstrating SSA in a spiking response with ISI of 200 ms and less adaptation as ISI is increased. (B) Firing rate of the neuron in part A to standard and deviant stimuli in all repeated trials (n = 5 trials, paired Student's t test, $p < 0.05$). (C) An example of a nonadapting neuron in MGB, which showed a similar amplitude of a spiking response to standard and deviant tones regardless of ISI. (D) Firing rate of the neuron in part C to standard and deviant stimuli in all repeated trials, bars indicate SD (n = 5 trials, paired Student's t test, $p > 0.05$).

to acoustic stimulation.[51,52] Previous studies found SSA in the MGM and MGD[22] and very low levels of SSA in the MGV.[22−24]

The thalamic reticular nucleus (TRN) is a major source of inhibitory inputs to MGB neurons in addition to inferior colliculus (IC) γ aminobutyric acid (GABAergic) neurons and local thalamic inhibitory neurons.[40] The TRN is a thin, shell-shaped nucleus composed of GABAergic neurons, located between the thalamus and the cortex so that all the fibers passing either way between thalamus and cortex pass through

https://doi.org/10.1021/acschemneuro.1c00137
ACS Chem. Neurosci. 2021, 12, 1688−1697

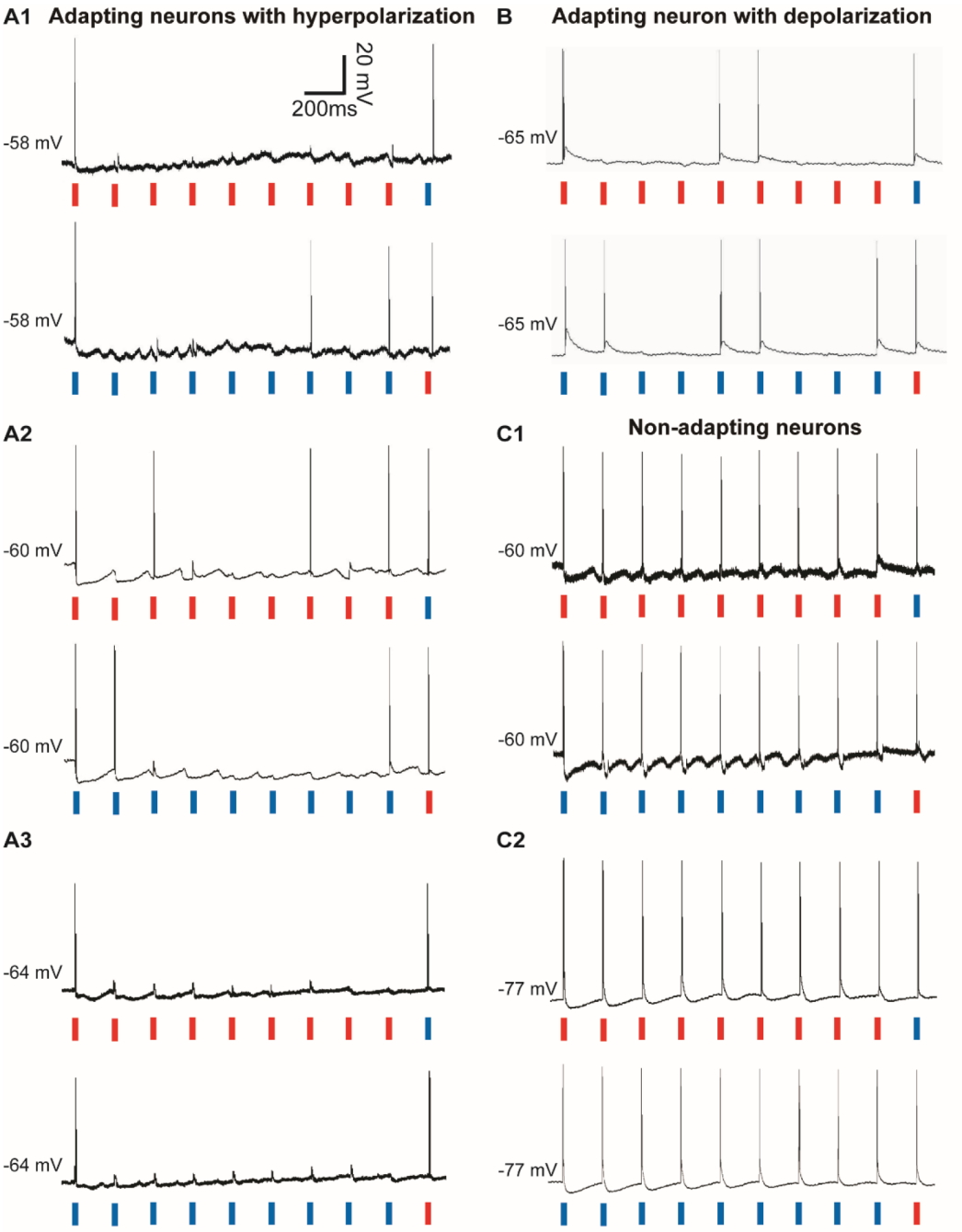

Figure 3. Adapting and nonadapting neurons at ISI of 200 ms. (A1−A3) Adapting neurons with inhibitory inputs. (B) Adapting neurons with excitatory inputs. Nonadapting neurons with inhibitory inputs (C1) and excitatory inputs (C2).

the TRN.[53−57] However, the TRN sends inhibitory projections only to MGD instead of the cortex,[57] which functions to modulate signals going through the thalamus and control the internal attentional searchlight.[56,57] In contrast to moderate SSA of MGB neurons, neurons in the auditory sector of the TRN exhibit stronger SSA.[22,23,27] In addition, previous studies showed that the response of TRN neurons to a deviant stimulus either enhanced or suppressed MGB neural responses to the succeeding auditory stimulus,[27] which suggests that the SSA of the TRN influences the sound processing of MGB neurons. However, it remains largely unknown whether and how the SSA of MGB neurons are modulated by the neural activities of the TRN. As the TRN sends only inhibitory projections to MGB neurons,[53−56,58,59] it is difficult to study TRN modulation of SSA of MGB neurons by extracellular recordings, which cannot detect the subthreshold membrane potential changes. In the current study, we used the intracellular recording to study the SSA of MGB neurons, especially those with long-lasting inhibitory inputs, and examine the SSA of those neurons before and after inactivation of the TRN.

RESULTS AND DISCUSSION

MGB Neurons Exhibit SSA at the Spiking Level. Intracellular recordings were performed in 49 MGB neurons of 18 anesthetized guinea pigs (Figure 1A). These neurons were

https://doi.org/10.1021/acschemneuro.1c00137
ACS Chem. Neurosci. 2021, 12, 1688−1697

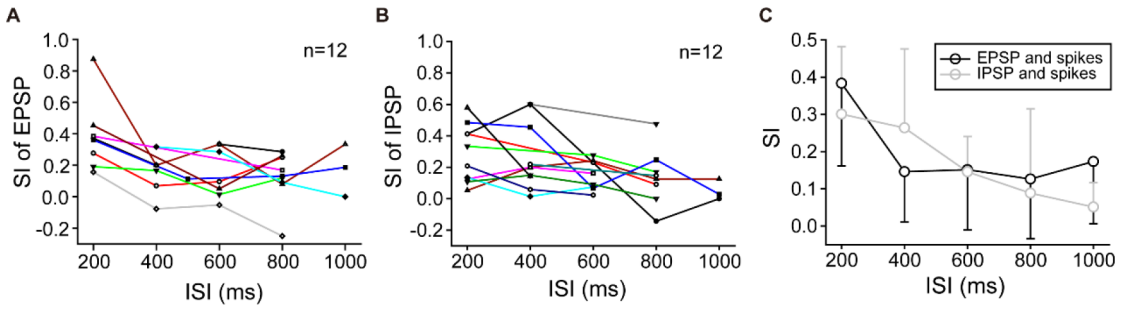

Figure 4. SSA index of MGB neurons with different subthreshold response. (A) SI of MGB neurons with EPSP and spikes. (B) SI of MGB neurons with IPSP and spikes. (C) Mean SI of these two types of neurons, bars indicate SD (n = 12, ANOVA with repeated measures, $p > 0.05$).

examined using a general oddball paradigm with a combination of two tones presented as standard and deviant stimuli, respectively (Figure 1B). The example MGB neuron responded to the first standard tone with spikes followed by long-lasting IPSPs, and thus, it adapted to subsequent standard tones as indicated by a decrease of spike response (Figure 2A, left). However, when a deviant tone was presented, the neuron showed a recuperative spike response and vice versa when the two tones were swapped. In contrast to the SSA with longer interstimulus intervals (ISIs), the SSA was strongest when the ISI was 200 ms. Decreased SSA occurred as the ISI was increased (Figure 2A, middle and right). The average spike response to deviant stimuli was significantly larger than the response to the same tone when presented as standard with an ISI of 200 ms (Figure 2B, n = 5 trials, unpaired Student's t test, $p < 0.05$). These neurons were identified as adapting neurons. Another group of MGB neurons responded robustly to the tone regardless of whether it was standard or deviant, even when the ISI was as short as 200 ms (Figure 2C). Additionally, for these MGB neurons, no significant difference of spike response was found between deviant and standard tones (Figure 2D, n = 5 trials, unpaired Student's t test, $p > 0.05$). These neurons were identified as nonadapting neurons.

Because SSA was stronger at a shorter ISI, we next examined the SSA of MGB neurons at an ISI of 200 ms (Figure 3). Notably, we observed the SSA at a spiking level for not only MGB neurons with excitatory inputs but also those with inhibitory inputs (Figure 3A,B). Some MGB neurons with inhibitory inputs did not show SSA even when the ISI was 200 ms (Figure 3C). We examined the SSA of MGB neurons with EPSP inputs (n = 12, Figure 4A) and IPSP inputs (n = 12, Figure 4B), respectively, via oddball stimuli with different ISIs and quantified them with the SSA index (SI; see Methods/Data Analysis sections). The SI of these two types of MGB neurons decreased with increasing ISIs and no significant difference of SI between these two types of MGB neurons (Figure 4C, n = 24, ANOVA with repeated measures, $p > 0.05$).

MGB Neurons with Long-Lasting IPSPs Exhibited an SSA at Subthreshold Levels. Some MGB neurons demonstrated long-lasting IPSPs without any spikes in response to acoustic stimuli. We found that the amplitude of hyperpolarization evoked by the first tone was larger than those evoked by succeeding tones when the ISI was 200 ms; however, this was not observed for an ISI of 1000 ms. For these MGB neurons, we presented oddball stimuli with a combination of two tones as standard and deviant stimuli, respectively. As shown in Figure 5B, the first standard tone elicited a large hyperpolarized response, and the subsequent standard tones elicited hyperpolarized responses with a smaller amplitude. However, when the deviant tone was presented, the example MGB neuron demonstrated an evoked subthreshold response with larger and longer-lasting IPSPs again, as indicated by the black arrow in the trace. We quantified the subthreshold response by area of hyperpolarization for standard and deviant tones, respectively. The area of hyperpolarized response to the deviant tone was significantly larger than that to the standard tones even when the ISI was 800 ms (Figure 5C, n = 4 trials, unpaired Student's t test, $p < 0.05$). These neurons showed a decrease in the SI of IPSPs, as the ISI was increased (Figure 5D, n = 5).

We recorded a total of 49 MGB neurons, which were examined by oddball stimuli. Of the neurons recorded, 37% (17/49) were nonadapting neurons, whereas 63% were adapting neurons. Among the adapting neurons, 26% (12/49) were those with depolarized response, while 26% (12/49) were those with a hyperpolarized response and spikes; meanwhile, 11% (5/49) were those with only a hyperpolarized response.

Long-Lasting IPSPs of MGB Neurons Originate from the Neural Activity of the TRN. Previous studies showed that the inhibitory inputs that MGB neurons receive have three different sources: IC GABAergic inhibitory neurons, MGB local inhibitory neurons, and the TRN.[40] We hypothesized that the long-lasting hyperpolarized response of MGB neurons originated mainly from the neural activity of the TRN. Extracellular recordings were conducted in the TRN simultaneously with intracellular recordings in the MGB to test this hypothesis. These simultaneous recordings showed that the long-lasting IPSPs of the MGB neurons synchronized with the burst firings of the TRN neurons (Figure 6A). Burst firings of the TRN neurons elicited by acoustic stimuli preceded the long-lasting hyperpolarized responses of MGB neurons by about 10 ms (Figure 6B, n = 6, paired Student's t test, $p < 0.001$). Next, we inactivated the neural activity of the TRN by microinjection of lidocaine, confirmed by the diminished burst firing of TRN neurons at the injection site. In this case, we found that long-lasting IPSPs of the MGB neuron in response to acoustic stimuli decreased after the TRN was inactivated (Figure 6C). Interestingly, the hyperpolarized response elicited by acoustic stimuli changed to small depolarized responses in the same MGB neuron recorded intracellularly. These results indicate that the long-lasting hyperpolarized response of MGB neurons originates from inhibitory inputs of the TRN.

SSA of MGB Neurons with Long-Lasting IPSPs Weakens after Inactivation of the TRN. Next, we examined whether the SSA of MGB neurons with long-lasting

https://doi.org/10.1021/acschemneuro.1c00137
ACS Chem. Neurosci. 2021, 12, 1688−1697

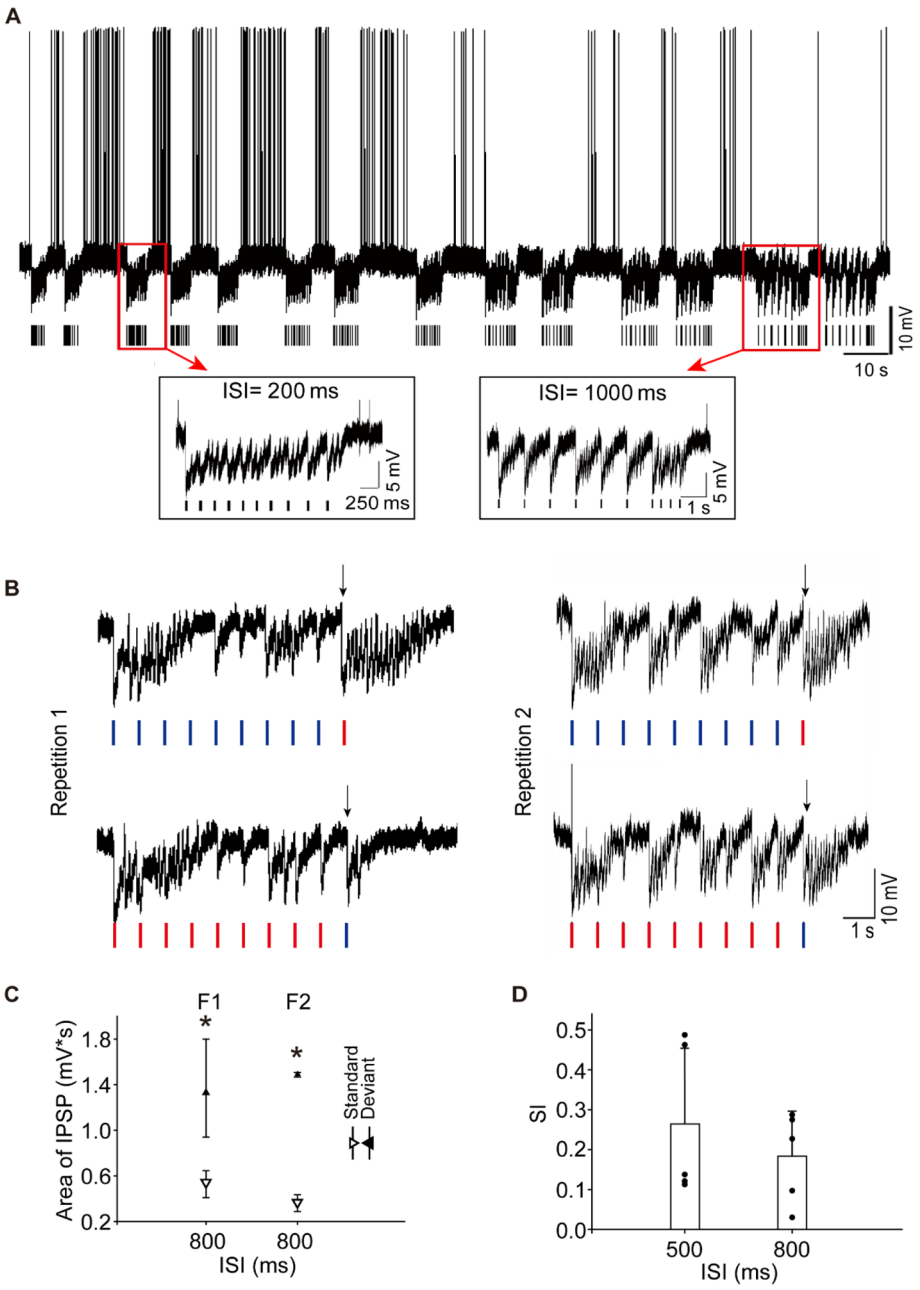

Figure 5. SSA of MGB neurons with long-lasting IPSPs. (A) An example MGB neuron exhibiting long-lasting IPSPs to repeated tone stimuli; traces in red boxes are enlarged at the bottom. (B) An example adapting neuron with long-lasting IPSPs. Responses to two repetitions of oddball stimuli at ISI 800 ms are presented. Black arrows indicate response to the deviant stimuli. (C) Normalized response amplitude of the long-lasting IPSPs to standard and deviant tone, respectively. F1 and F2 represent tones with different frequencies (n = 4 trials, paired Student's t test, $p < 0.05$). (D) SI of MGB neurons with IPSPs (n = 5) in response to oddball stimuli at ISIs of 500 and 800 ms, respectively.

IPSPs was affected by the neural activity of the TRN. We tested the SSA of MGB neurons with oddball stimuli before and after TRN inactivation. Similar to the results above, long-lasting IPSPs of the example MGB neuron were synchronized to the burst firings of TRN neurons (Figure 7A). When oddball stimuli were presented, the example MGB neuron demonstrated strong adaptation to the repeated standard tones as indicated by a decreased spiking response (Figure 7A). The firing pattern of the example MGB neuron changed from hyperpolarized response to depolarized response with spikes, and the SSA of this neuron weakened as indicated by robust spikes to both the standard and deviant stimuli, after the TRN was inactivated (Figure 7B). The firing rate of the MGB neuron significantly increased (Figure 7C, n = 5 trials, unpaired Student's t test, $P < 0.01$). Moreover, the averaged spike response to the deviant tone was slightly lower than that to the standard tone after TRN inactivation. The result revealed that the SSA of MGB neurons weakened after the TRN was inactivated, as shown by the SSA index, SI (Figure 7D, 0.56 ± 0.35 vs -0.21 ± 0.42, n = 5 trials, unpaired Student's t test, $P < 0.05$).

In the present study, we applied intracellular recordings to examine the SSA of MGB neurons with inhibitory inputs at both spike and subthreshold levels in anesthetized guinea pigs. We further investigated the circuit mechanism underlying the SSA of MGB neurons by using microinjection of lidocaine to

https://doi.org/10.1021/acschemneuro.1c00137
ACS Chem. Neurosci. 2021, 12, 1688−1697

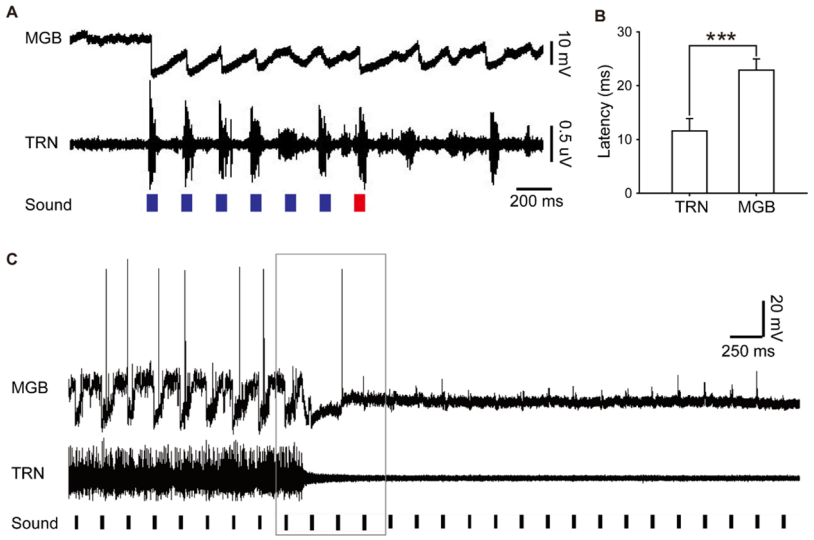

Figure 6. Long-lasting IPSPs of MGB neurons diminished after inactivation of TRN. (A) Simultaneous recordings in the MGB (intracellular recording, upper trace) and TRN (extracellular recording, middle trace) to oddball acoustic stimuli (lower trace). Different colors represent tones with different frequencies. (B) Onset response latencies of TRN and MGB neurons to tone stimuli ($n = 6$, paired Student's t test, $p < 0.001$). (C) Long-lasting IPSPs of the example MGB neuron diminished after inactivation of TRN by microinjection of lidocaine. The data presentation is the same as that of part A. The rectangle indicates the time window of microinjection.

inactivate the neural activity of the TRN. In contrast to previous studies, our intracellular recordings reveal that MGB neurons with long-lasting IPSPs have an SSA not only at the spiking level but also at the subthreshold level. We also showed that these long-lasting hyperpolarized responses originated from neural activities of the TRN. Moreover, inactivation of the TRN resulted in a change of response pattern of MGB neurons and thus weakened the SSA of the MGB neurons.

The SSA is important for mammals to detect a novel object or sensory stimulus. It is especially important in the auditory system, where the SSA is strong and widespread. Previous studies have shown that the SSA in subcortical stations is linked to the nonlemniscal pathway and is mostly absent in the lemniscal pathway.[8] The primary auditory cortex (A1) is the first lemniscal station where the SSA is widespread.[7,29] Taking inferior colliculus (IC) as an example, SSA was found in the external nucleus and dorsal regions of the IC, and a low level of SSA was found in the central nucleus of the IC.[9,12] Extracellular recordings in MGB showed that neurons in the medial and dorsal subdivisions (nonlemniscal pathway) showed a stronger SSA than that of neurons in the ventral division (lemniscal pathway).[22,23,27] In this study, we found that a substantial proportion of MGB neurons with long-lasting hyperpolarized membrane potential showed adaptation at both the spiking and subthreshold levels. The MGB neurons we recorded are most likely located in the nonlemniscal pathway as previous studies revealed that both the dorsal and medial thalamus receive inhibitory inputs from the TRN through the corticothalamic loop.[58−61] Thus, our results confirm the view that the SSA in the subcortical levels is linked to the nonlemniscal pathway. So far, the mechanisms underlying the SSA remain unclear. It is believed that synaptic depression plays an important role in the generation of SSA at the spiking level, whether on the feedforward path or in recurrent circuits.[62] In the current study, we found that the SSA of MGB neurons is dependent on the ISI, which supports the view that synaptic depression underlies the generation of SSA. Moreover, we found that the SSA of MGB neurons is modulated by long-lasting inhibitory inputs from the TRN, revealing an alternative circuity mechanism underlying the SSA.

In contrast to that of the MGB, TRN neurons showed a stronger SSA, which was stimulus specific.[27,28] A previous study found that deviance detection in TRN neurons could either enhance or suppress MGB neuronal responses following auditory stimulus.[27] The deviance detection feature of the TRN was proposed to induce an attention shift to a novel stimulus at the dorsal thalamus, echoing the old "searchlight" hypothesis by Crick.[63] In the present study, we performed intracellular recordings in MGB neurons to examine whether and how SSA in MGB neurons is affected by inhibitory inputs from the TRN, a question that cannot be answered using extracellular recordings. Our study shows that the SSA of MGB neurons with long-lasting hyperpolarized membrane potentials is altered after inactivation of the TRN, via which the cortex implements the corticofugal inhibitory control. Several other studies have examined whether the SSA observed in the MGB originates from the auditory cortex, possibly as a higher-order sensory process transmitted to subcortical nuclei in a top-down manner.[21,24,34,64] On one hand, cortical inactivation by application of the $GABA_A$ agonist indicates that SSA in the ventral division of the MGB is mainly regulated by the corticofugal system,[24] which sheds light on the view that the SSA of the MGB may originate from the auditory cortex.[34] On the other hand, another study showed that the SSA of MGB neurons was not altered after cooling the auditory cortex of an anesthetized rat.[21] Because the cortical neurons of the anesthetized rat were already suppressed, further studies may be necessary to examine the corticofugal modulation effect on the SSA of MGB neurons in behavioral animals via cortical inactivation through implanted drug cannula.

In summary, our study reveals the SSA at both the spiking and subthreshold levels in MGB neurons with long-lasting hyperpolarized responses. Simultaneous extracellular recordings in the TRN indicate that the long-lasting hyperpolarized response of MGB neurons originates from the activity of TRN

https://doi.org/10.1021/acschemneuro.1c00137
ACS Chem. Neurosci. 2021, 12, 1688−1697

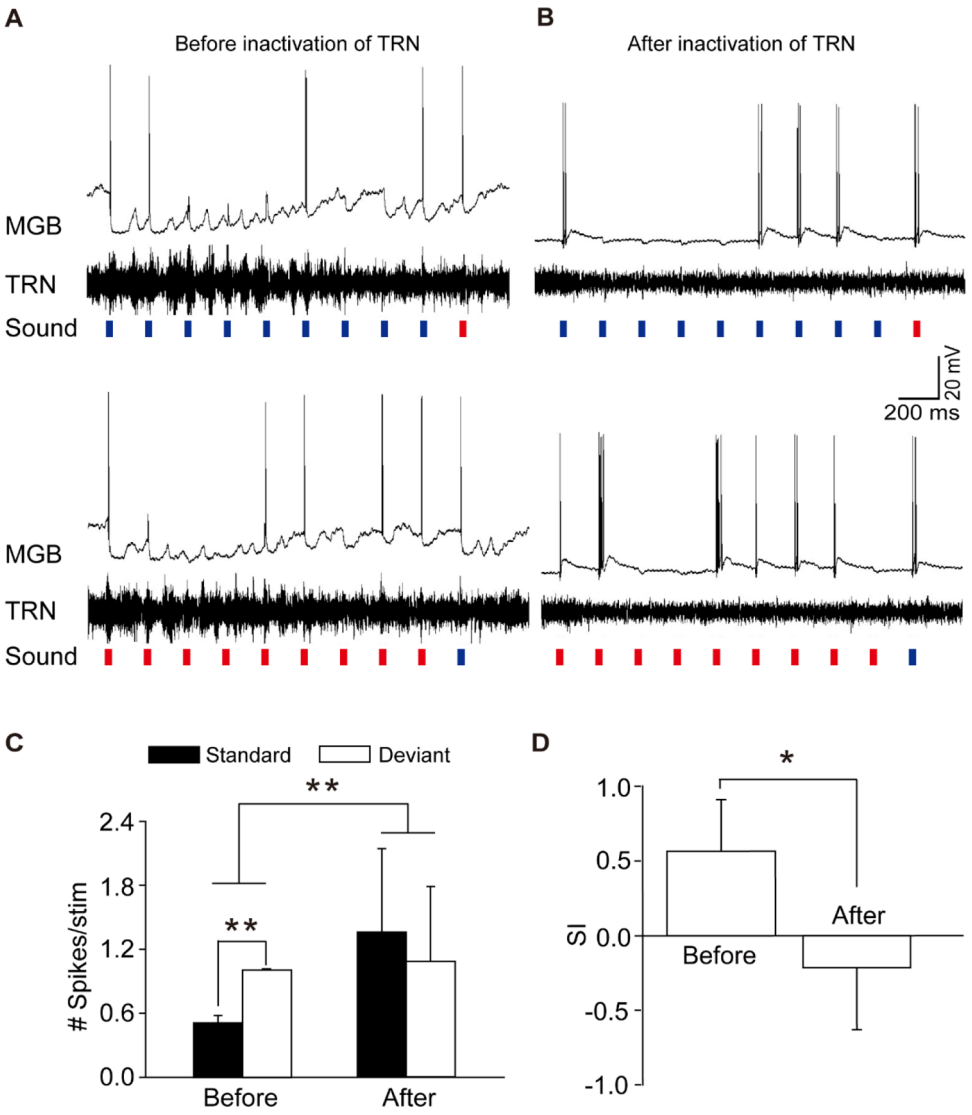

Figure 7. SSA of MGB neurons weakened after inactivation of TRN. Simultaneous recordings in the MGB (intracellular recording, Top) and TRN (extracellular recording, Middle) to oddball acoustic stimuli (Bottom) before (A) and after (B) inactivation of TRN. Responses to two oddball sequences are presented in each plot. (C) Firing rate of the example MGB neuron in response to oddball stimuli at ISI of 200 ms before and after inactivation of the TRN (n = 3 trials, unpaired Student's t test, $P < 0.01$). (D) SI of the example MGB neuron before and after inactivation of the TRN (n = 3 trials, unpaired Student's t test, $P < 0.05$).

neurons. Most of the long-lasting hyperpolarized responses of MGB neurons were diminished, and thus, the SSA with inhibitory inputs was weakened in the MGB after the TRN was inactivated. Our results suggested that the SSA in the MGB was strongly modulated by the inhibitory inputs from the TRN, which offers an alternative circuit mechanism of SSA in the auditory thalamus.

METHODS

Procedures. All experimental procedures were approved by the Hong Kong Polytechnic University Animal Care and Use Committee as well as the Zhejiang University Animal Care and Use Committee.

Animals. Eighteen adult guinea pigs (8−10 weeks, 350−700 g) of both sexes were used.

Surgical Procedure. Animals were initially anaesthetized with pentobarbital sodium (Nembutal, Abbott, 40 mg/kg, i.p.) and maintained by the same anesthetic (5−10 mg/kg/h, i.p.) during the surgical procedure and recording. Details of animal preparation for intracellular recordings were the same as those described previously.[52,60] In brief, the animal was paralyzed with Gallamine Triethiodide (initially 50 mg/kg, maintained at 5−10 mg/kg/h, i.m.) and artificially ventilated. After the animal subjects were mounted in a stereotaxic device, a craniotomy was made to allow for access of the MGB in the right hemisphere. Cerebrospinal fluid was released at the medulla level. Throughout the intracellular recording experiment, an electroencephalogram (EEG) was continuously monitored to assess the level of anesthesia. The body temperature of the animals was maintained at 37−38 °C.

Intracellular Recordings. Intracellular recordings from MGB neurons were performed using glass micropipettes filled with 3.0 M KAc (pH 7.6). The pipet resistance was 40−90 MΩ. The electrode was advanced vertically with a motorized manipulator (DM 1510, Narishige). After the electrode was inserted to a depth of 4−5 mm, the cortical exposure was sealed with low melting point paraffin. When the electrode was moved to the desired depth above the MGB, it was slowly advanced by 4 μm steps. Brief capacitance over-compensation (30 ms) was applied to generate a small vibration of the electrode tip, which facilitated the penetration of the cell membrane and displayed an immediate drop of the recorded potential. After the micropipette was stabilized for a few seconds inside the cell, we started to play sounds and record the membrane

https://doi.org/10.1021/acschemneuro.1c00137
ACS Chem. Neurosci. 2021, 12, 1688−1697

potentials and firing patterns of recorded neurons. The electrical signals were amplified by an amplifier (Axon 2B, Molecular Devices), digitized (Digidata 1322A, Molecular Devices), and stored in the computer using AxoScope software (Axoscope 9.0, Molecular Devices). Data from neurons with a resting membrane potential lower than −50 mV were used.

Extracellular Recordings. Tungsten microelectrodes with impedances of 2−7 MΩ (Frederick Haer) were used to record the neural activity of the TRN accessed from the top of the brain. The vertical coordinate of the electrode was measured from a point slightly above the cortical surface. The signal recorded by the microelectrode, together with the acoustic stimulus signal, was amplified by OpenEX (Tucker-Davis Technologies) and stored by Axoscope software (Axoscope 9.0, Molecular Devices).

Acoustic Stimuli. The experiments were performed in a double-wall sound-proofed chamber. Acoustic stimuli were generated digitally by a computer-controlled auditory workstation (Tucker-Davis Technologies system) and delivered to the left ear of the subjects via a coupled electrostatic speaker (EC1, Tucker-Davis Technologies) through a hollow ear bar. The sound pressure level (SPL) of the output was calibrated over the frequency range 100−35 kHz with a condenser microphone (Center Technology). Repeated noise bursts (50 dB SPL, 5 ms rise/fall time, 100 ms in duration, 1000 ms interval) were used to search for MGB neurons. A frequency tuning curve of the recorded neurons was examined by scanning pure tones at different frequencies (50 dB SPL, 5 ms rise/fall time, 100 ms in duration, 500 ms interval, and 5 repetitions at each frequency) before a specific oddball paradigm was set for each neuron.

Oddball Procedure. To examine the SSA of MGB neurons, we selected two frequencies, f1 and f2 (f1 < f2), with the central frequency (f2 × f1)1/2 having a fixed value close to the BF of the recorded neuron. Stimulus intensity was set to 50 dB. We presented a block of pure-tone stimuli consisting of f1, f1, ...f1, f1, and f2. Then, f1 and f2 were swapped (f2, f2, ...f2, f2 and f1), as shown in Figure 1B. In most cases, the standard and deviant stimuli occurred at a pulse number ratio of 9:1. Otherwise, this ratio was 6:1, as specified. Each set of the above stimuli was repeated 5−10 times. In addition, as most neurons in the MGB did not show SSA when the ISI was 1000 ms, we varied the interstimulus interval (ISI) systematically in the range 1000−200 ms by 200 ms steps. In a few cases, ISI values were 800 and 500 ms, respectively.

Inactivation of the TRN. Neural activity of the TRN was deactivated by microinjection of lidocaine (0.3−0.5 μL/20 mg/mL) which was administered in nine animals using a microinjection system (Hamilton). A tungsten microelectrode was glued to the injection glass pipet to monitor the neural activity of the TRN. The distance between the two tips was approximately 200 μm.

Data Analysis. Neuronal signals were continuously digitized and saved onto a computer storage drive during each stimulus presentation. Both the membrane potential and spike data were analyzed offline using pCLAMP 9.0 (Molecular Devices). Spikes were detected online by setting a threshold of at least 30 mV above the baseline of the membrane potential using custom software implemented in Matlab (Mathworks). The magnitude of the subthreshold response was measured by the area of depolarization or hyperpolarization over the stimulus duration. The spiking or subthreshold responses to all nine stimuli in the standard-stimulus train were first averaged together and then further averaged among repetitions. Data were averaged if there were multiple repetitions. All values are expressed as mean ± SD unless otherwise specified. Differences between standard and deviant stimuli were analyzed with an unpaired Student's t test. Results obtained before and after inactivation of the TRN were analyzed with ANOVA. The p values with $p < 0.0001$, $p < 0.001$, $p < 0.01$, or $p < 0.05$ were considered statistically significant in respective tests, as indicated where appropriate.

The SSA index for each frequency was used as the frequency-specific index SI (fi), which was calculated using the equation $SI(fi) = (D(fi) - S(fi))/(D(fi) + S(fi))$, where $D(fi)$ and $S(fi)$ were spiking responses to the deviant and standard frequency, respectively.

AUTHOR INFORMATION

Corresponding Authors

Lixia Gao − *Department of Neurology of the Second Affiliated Hospital and Interdisciplinary Institute of Neuroscience and Technology, Zhejiang University School of Medicine, Hangzhou 310029, China; Department of Rehabilitation Sciences, The Hong Kong Polytechnic University, Hung Hom, Kowloon, Hong Kong; Key Laboratory of Biomedical Engineering of Ministry of Education, College of Biomedical Engineering and Instrument Science, Zhejiang University, Hangzhou 310027, China;* orcid.org/0000-0002-1884-0257; Phone: 86-0571-8697-1646; Email: lxgao10@zju.edu.cn

Jufang He − *Department of Rehabilitation Sciences, The Hong Kong Polytechnic University, Hung Hom, Kowloon, Hong Kong; Departments of Neuroscience and Biomedical Sciences, City University of Hong Kong, Kowloon Tong, Hong Kong;* Phone: 3442 7042; Email: jufanghe@cityu.edu.hk

Authors

Guoqiang Jia − *Department of Neurology of the Second Affiliated Hospital and Interdisciplinary Institute of Neuroscience and Technology, Zhejiang University School of Medicine, Hangzhou 310029, China*

Xinjian Li − *Department of Neurology of the Second Affiliated Hospital and Interdisciplinary Institute of Neuroscience and Technology, Zhejiang University School of Medicine, Hangzhou 310029, China; Department of Rehabilitation Sciences, The Hong Kong Polytechnic University, Hung Hom, Kowloon, Hong Kong*

Chunhua Liu − *Department of Rehabilitation Sciences, The Hong Kong Polytechnic University, Hung Hom, Kowloon, Hong Kong; Guangzhou Regenerative Medicine and Health Guang Dong Laboratory, Guangzhou 510005, China*

Complete contact information is available at: https://pubs.acs.org/10.1021/acschemneuro.1c00137

Notes

The authors declare no competing financial interest.

ACKNOWLEDGMENTS

This work was supported by the National Key R&D Program of China (2018YFC1005003), the Natural Science Foundation of China (31871056, 61703365, 91732302), the Fundamental Research Funds for the Central Universities (2018QN81008), the Hong Kong Research Grants Council, the General Research Fund (11102417, 11166316, 14117319, 5611/11M), the Innovation and Technology Fund (MRP/053/18X, MRP/101/17X, GHP_075_19GD), and the Health and Medical Research Fund (06172456, 31571096).

REFERENCES

(1) Katz, Y., Heiss, J. E., and Lampl, I. (2006) Cross-whisker adaptation of neurons in the rat barrel cortex. *J. Neurosci. 26*, 13363−13372.

(2) Muller, J. R., Metha, A. B., Krauskopf, J., and Lennie, P. (1999) Rapid adaptation in visual cortex to the structure of images. *Science 285*, 1405−1408.

(3) Tonosaki, K. (2004) Cross-adaptation to odor stimulation of olfactory receptor cells in the box turtle, Terrapene carolina. *Brain Behav Evol 41*, 187−191.

(4) Baylis, G. C., and Rolls, E. T. (1987) Responses of neurons in the inferior temporal cortex in short term and serial recognition memory tasks. *Exp. Brain Res. 65*, 614−622.
(5) Reches, A., Netser, S., and Gutfreund, Y. (2010) Interactions between Stimulus-Specific Adaptation and Visual Auditory Integration in the Forebrain of the Barn Owl. *J. Neurosci. 30*, 6991−6998.
(6) Perez-Gonzalez, D., Malmierca, M. S., and Covey, E. (2005) Novelty detector neurons in the mammalian auditory midbrain. *Eur. J. Neurosci 22*, 2879−2885.
(7) Ulanovsky, N., Las, L., and Nelken, I. (2003) Processing of low-probability sounds by cortical neurons. *Nat. Neurosci. 6*, 391−398.
(8) Nelken, I. (2014) Stimulus-specific adaptation and deviance detection in the auditory system: experiments and models. *Biological cybernetics 108*, 655−663.
(9) Malmierca, M. S., Cristaudo, S., Perez-Gonzalez, D., and Covey, E. (2009) Stimulus-specific adaptation in the inferior colliculus of the anesthetized rat. *J. Neurosci. 29*, 5483−5493.
(10) Ayala, Y. A., and Malmierca, M. S. (2013) Stimulus-specific adaptation and deviance detection in the inferior colliculus. *Front. Neural Circuits 6*, 89.
(11) Ayala, Y. A., Perez-Gonzalez, D., Duque, D., Nelken, I., and Malmierca, M. S. (2013) Frequency discrimination and stimulus deviance in the inferior colliculus and cochlear nucleus. *Front. Neural Circuits 6*, 119.
(12) Duque, D., Perez-Gonzalez, D., Ayala, Y. A., Palmer, A. R., and Malmierca, M. S. (2012) Topographic distribution, frequency, and intensity dependence of stimulus-specific adaptation in the inferior colliculus of the rat. *J. Neurosci. 32*, 17762−17774.
(13) Lumani, A., and Zhang, H. (2010) Responses of neurons in the rat's dorsal cortex of the inferior colliculus to monaural tone bursts. *Brain Res. 1351*, 115−129.
(14) Perez-Gonzalez, D., Hernandez, O., Covey, E., and Malmierca, M. S. (2012) GABA(A)-mediated inhibition modulates stimulus-specific adaptation in the inferior colliculus. *PLoS One 7*, e34297.
(15) Perez-Gonzalez, D., and Malmierca, M. S. (2012) Variability of the time course of stimulus-specific adaptation in the inferior colliculus. *Front. Neural Circuits 6*, 107.
(16) Ayala, Y. A., and Malmierca, M. S. (2015) Cholinergic Modulation of Stimulus-Specific Adaptation in the Inferior Colliculus. *J. Neurosci. 35*, 12261−12272.
(17) Ayala, Y. A., Perez-Gonzalez, D., and Malmierca, M. S. (2016) Stimulus-specific adaptation in the inferior colliculus: The role of excitatory, inhibitory and modulatory inputs. *Biol. Psychol. 116*, 10.
(18) Ayala, Y. A., Udeh, A., Dutta, K., Bishop, D., Malmierca, M. S., and Oliver, D. L. (2015) Differences in the strength of cortical and brainstem inputs to SSA and non-SSA neurons in the inferior colliculus. *Sci. Rep. 5*, 10383.
(19) Duque, D., and Malmierca, M. S. (2015) Stimulus-specific adaptation in the inferior colliculus of the mouse: anesthesia and spontaneous activity effects. *Brain Struct. Funct. 220*, 3385−3398.
(20) Kraus, N., McGee, T., Littman, T., Nicol, T., and King, C. (1994) Nonprimary auditory thalamic representation of acoustic change. *J. Neurophysiol. 72*, 1270−1277.
(21) Antunes, F. M., and Malmierca, M. S. (2011) Effect of auditory cortex deactivation on stimulus-specific adaptation in the medial geniculate body. *J. Neurosci. 31*, 17306−17316.
(22) Antunes, F. M., Nelken, I., Covey, E., and Malmierca, M. S. (2010) Stimulus-specific adaptation in the auditory thalamus of the anesthetized rat. *PLoS One 5*, e14071.
(23) Anderson, L. A., Christianson, G. B., and Linden, J. F. (2009) Stimulus-specific adaptation occurs in the auditory thalamus. *J. Neurosci. 29*, 7359−7363.
(24) Bauerle, P., von der Behrens, W., Kossl, M., and Gaese, B. H. (2011) Stimulus-specific adaptation in the gerbil primary auditory thalamus is the result of a fast frequency-specific habituation and is regulated by the corticofugal system. *J. Neurosci. 31*, 9708−9722.
(25) Richardson, B. D., Hancock, K. E., and Caspary, D. M. (2013) Stimulus-specific adaptation in auditory thalamus of young and aged awake rats. *J. Neurophysiol. 110*, 1892−1902.
(26) Malmierca, M. S., Anderson, L. A., and Antunes, F. M. (2015) The cortical modulation of stimulus-specific adaptation in the auditory midbrain and thalamus: a potential neuronal correlate for predictive coding. *Front. Syst. Neurosci. 9*, 19.
(27) Yu, X. J., Xu, X. X., He, S., and He, J. (2009) Change detection by thalamic reticular neurons. *Nat. Neurosci. 12*, 1165−1170.
(28) Yu, X. J., Xu, X. X., Chen, X., He, S., and He, J. (2009) Slow recovery from excitation of thalamic reticular nucleus neurons. *J. Neurophysiol. 101*, 980−987.
(29) Ulanovsky, N., Las, L., Farkas, D., and Nelken, I. (2004) Multiple time scales of adaptation in auditory cortex neurons. *J. Neurosci. 24*, 10440−10453.
(30) Taaseh, N., Yaron, A., and Nelken, I. (2011) Stimulus-specific adaptation and deviance detection in the rat auditory cortex. *PLoS One 6*, e23369.
(31) Farley, B. J., Quirk, M. C., Doherty, J. J., and Christian, E. P. (2010) Stimulus-specific adaptation in auditory cortex is an NMDA-independent process distinct from the sensory novelty encoded by the mismatch negativity. *J. Neurosci. 30*, 16475−16484.
(32) Nelken, I., and Ulanovsky, N. (2007) Mismatch negativity and stimulus-specific adaptation in animal models. *J. Psychophysiol 21*, 214−223.
(33) Szymanski, F. D., Garcia-Lazaro, J. A., and Schnupp, J. W. (2009) Current source density profiles of stimulus-specific adaptation in rat auditory cortex. *J. Neurophysiol. 102*, 1483−1490.
(34) von der Behrens, W., Bauerle, P., Kossl, M., and Gaese, B. H. (2009) Correlating stimulus-specific adaptation of cortical neurons and local field potentials in the awake rat. *J. Neurosci. 29*, 13837−13849.
(35) Klein, C., von der Behrens, W., and Gaese, B. H. (2014) Stimulus-specific adaptation in field potentials and neuronal responses to frequency-modulated tones in the primary auditory cortex. *Brain topography 27*, 599−610.
(36) Nir, Y., Vyazovskiy, V. V., Cirelli, C., Banks, M. I., and Tononi, G. (2015) Auditory responses and stimulus-specific adaptation in rat auditory cortex are preserved across NREM and REM sleep. *Cereb Cortex 25*, 1362−1378.
(37) Winer, J. A., Wenstrup, J. J., and Larue, D. T. (1992) Patterns of GABAergic immunoreactivity define subdivisions of the mustached bat's medial geniculate body. *J. Comp. Neurol. 319*, 172−190.
(38) He, J. (2001) On and off pathways segregated at the auditory thalamus of the guinea pig. *J. Neurosci. 21*, 8672−8679.
(39) He, J. (2003) Corticofugal modulation on both ON and OFF responses in the nonlemniscal auditory thalamus of the guinea pig. *J. Neurophysiol. 89*, 367−381.
(40) He, J. (2003) Corticofugal modulation of the auditory thalamus. *Exp. Brain Res. 153*, 579−590.
(41) Calford, M. B., and Aitkin, L. M. (1983) Ascending projections to the medial geniculate body of the cat: evidence for multiple, parallel auditory pathways through thalamus. *J. Neurosci. 3*, 2365−2380.
(42) Redies, H., Brandner, S., and Creutzfeldt, O. D. (1989) Anatomy of the auditory thalamocortical system of the guinea pig. *J. Comp. Neurol. 282*, 489−511.
(43) He, J. (2002) OFF responses in the auditory thalamus of the guinea pig. *J. Neurophysiol. 88*, 2377−2386.
(44) He, J., and Hashikawa, T. (1998) Connections of the dorsal zone of cat auditory cortex. *J. Comp. Neurol. 400*, 334−348.
(45) Bartlett, E. L., and Wang, X. (2011) Correlation of neural response properties with auditory thalamus subdivisions in the awake marmoset. *J. Neurophysiol. 105*, 2647−2667.
(46) Calford, M. B., and Webster, W. R. (1981) Auditory representation within principal division of cat medial geniculate body: an electrophysiology study. *J. Neurophysiol. 45*, 1013−1028.
(47) Imig, T. J., and Morel, A. (1983) Organization of the thalamocortical auditory system in the cat. *Annu. Rev. Neurosci. 6*, 95−120.

https://doi.org/10.1021/acschemneuro.1c00137
ACS Chem. Neurosci. 2021, 12, 1688−1697

(48) Winer, J. A., and Morest, D. K. (1983) The neuronal architecture of the dorsal division of the medial geniculate body of the cat. A study with the rapid Golgi method. *J. Comp. Neurol. 221*, 1−30.
(49) Hu, B. (1995) Cellular basis of temporal synaptic signalling: an in vitro electrophysiological study in rat auditory thalamus. *J. Physiol. 483* (Pt 1), 167−182.
(50) Mooney, D. M., Zhang, L., Basile, C., Senatorov, V. V., Ngsee, J., Omar, A., and Hu, B. (2004) Distinct forms of cholinergic modulation in parallel thalamic sensory pathways. *Proc. Natl. Acad. Sci. U. S. A. 101*, 320−324.
(51) Zhang, Z., Yu, Y. Q., Liu, C. H., Chan, Y. S., and He, J. (2008) Reprint of ″frequency tuning and firing pattern properties of auditory thalamic neurons: an in vivo intracellular recording from the guinea pig″ [Neuroscience 151 (2008) 293−302]. *Neuroscience 154*, 273−282.
(52) Xiong, Y., Yu, Y. Q., Chan, Y. S., and He, J. (2004) Effects of cortical stimulation on auditory-responsive thalamic neurones in anaesthetized guinea pigs. *J. Physiol. 560*, 207−217.
(53) Crabtree, J. W. (1998) Organization in the auditory sector of the cat's thalamic reticular nucleus. *J. Comp. Neurol. 390*, 167−182.
(54) Houser, C. R., Vaughn, J. E., Barber, R. P., and Roberts, E. (1980) GABA neurons are the major cell type of the nucleus reticularis thalami. *Brain Res. 200*, 341−354.
(55) Winer, J. A., and Larue, D. T. (1987) Patterns of reciprocity in auditory thalamocortical and corticothalamic connections: study with horseradish peroxidase and autoradiographic methods in the rat medial geniculate body. *J. Comp. Neurol. 257*, 282−315.
(56) Cotillon-Williams, N., Huetz, C., Hennevin, E., and Edeline, J. M. (2008) Tonotopic control of auditory thalamus frequency tuning by reticular thalamic neurons. *J. Neurophysiol. 99*, 1137−1151.
(57) Pinault, D. (2004) The thalamic reticular nucleus: structure, function and concept. *Brain Res. Rev. 46*, 1−31.
(58) Zhang, Z., Liu, C. H., Yu, Y. Q., Fujimoto, K., Chan, Y. S., and He, J. (2008) Corticofugal projection inhibits the auditory thalamus through the thalamic reticular nucleus. *J. Neurophysiol. 99*, 2938−2945.
(59) Gao, L., Meng, X., Ye, C., Zhang, H., Liu, C., Dan, Y., Poo, M. M., He, J., and Zhang, X. (2009) Entrainment of slow oscillations of auditory thalamic neurons by repetitive sound stimuli. *J. Neurosci. 29*, 6013−6021.
(60) Yu, Y. Q., Xiong, Y., Chan, Y. S., and He, J. (2004) Corticofugal gating of auditory information in the thalamus: an in vivo intracellular recording study. *J. Neurosci. 24*, 3060−3069.
(61) Yu, Y. Q., Xiong, Y., Chan, Y. S., and He, J. (2004) In vivo intracellular responses of the medial geniculate neurones to acoustic stimuli in anaesthetized guinea pigs. *J. Physiol. 560*, 191−205.
(62) Wehr, M., and Zador, A. M. (2005) Synaptic mechanisms of forward suppression in rat auditory cortex. *Neuron 47*, 437−445.
(63) Crick, F. (1984) Function of the thalamic reticular complex: the searchlight hypothesis. *Proc. Natl. Acad. Sci. U. S. A. 81*, 4586−4590.
(64) Villa, A. E., Rouiller, E. M., Simm, G. M., Zurita, P., de Ribaupierre, Y., and de Ribaupierre, F. (1991) Corticofugal modulation of the information processing in the auditory thalamus of the cat. *Exp. Brain Res. 86*, 506−517.

https://doi.org/10.1021/acschemneuro.1c00137
ACS Chem. Neurosci. 2021, 12, 1688−1697